ACS APPLIED MATERIALS & INTERFACES

Research Article

www.acsami.org

Heteropolyacid-Functionalized Aluminum 2-Aminoterephthalate Metal-Organic Frameworks As Reactive Aldehyde Sorbents and Catalysts

Lev Bromberg, Xiao Su, and T. Alan Hatton*

Department of Chemical Engineering, Massachusetts Institute of Technology, Cambridge, Massachusetts 02139, United States

Supporting Information

ABSTRACT: Porous materials based on aluminum(III) 2-aminoterephthalate metal organic frameworks (MOFs NH_2MIL101(Al) and NH_2MIL53(Al)) and their composites with phosphotungstic acid (PTA) were studied as sorbents of saturated vapors of acetaldehyde, acrolein, and butyraldehyde. MOF functionalization by PTA impregnation from aqueous/methanol solutions resulted in MOF with the original crystal topology with the presence of an ordered PTA phase in the MOF/PTA composite. The MOF/PTA composites contained 29−32 wt % PTA and were stable against loss of PTA through leaching to the aqueous/organic solvent solutions. The MOF and MOF/PTA materials exhibited equilibrium uptake of acetaldehyde from its saturated vapor phase exceeding 50 and 600 wt %, respectively, at 25 °C. The acetaldehyde vapor uptake occurs through the vapor condensation, pore-filling mechanism with simultaneous conversion of acetaldehyde to crotonaldehyde and higher-molecular-weight compounds resulting from repeated aldol condensation. The products of aldehyde condensation and polymerization were identified by MALDI-TOF and electrospray mass spectrometry. The kinetics of the MOF- and MOF/PTA-catalyzed aldol condensation of acetaldehyde were studied in water−acetonitrile mixtures. The aldol condensation kinetics in MOF suspensions were rapid and pseudo-first-order. The apparent second-order rate constants for the aldol condensation catalyzed by MOF/PTA were estimated to be 5×10^{-4} to 1.5×10^{-3} $M^{-1}s^{-1}$, which are higher than those reported in the case of homogeneous catalysis by amino acids or sulfuric acid. MOF and MOF/PTA materials are efficient heterogeneous catalysts for the aldehyde self-condensation in aqueous−organic media.

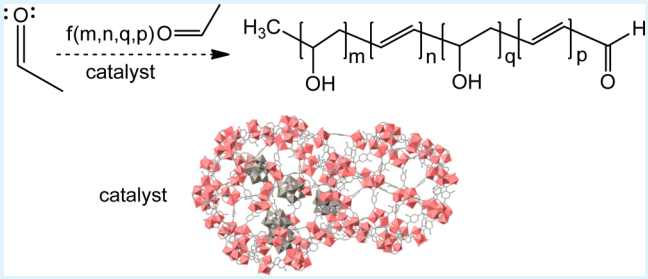

KEYWORDS: *aluminum 2-aminoterephthalate, phosphotungstic acid, metal−organic framework, composite, aldehyde condensation, acrolein polymerization, catalysis*

INTRODUCTION

The potential for metal−organic frameworks (MOFs) as sorbents and matrices in heterogeneous catalysis stems from their high crystallinity, thermal and chemical stability, high porosity allowing for rapid mass transport, desirable interactions with substrates, and tunability of the active sites.[1−9] MOFs can act as heterogeneous catalysts either through their coordinatively unsaturated metal centers, or by functional groups incorporated in the linkers and/or attached to their metal centers through direct synthesis or by postsynthetic modification.[10−13] Despite these desirable features, there are few reports on MOF-based reactive sorbents and catalysts for the chemical conversion of aldehydes.[14,15] Yet, volatile aldehydes are common constituents of both indoor and outdoor air produced by incomplete combustion of organic materials, oxidation of atmospheric chemicals such as components of vehicle exhausts, volatilization of heated cooking oil, cigarette smoke, incense, candles, wood-burning fireplaces, etc.[16−19] Thus far, activated carbons have proven to be inefficient as aldehyde vapor sorbents, while recent trends in carbon dioxide capture developments indicate interest in the amine-supported sorbents synthesized by the immobilization of amines into mesoporous supports via postgrafting, wet impregnation and co-condensation of aminosilanes, tetraalkoxysilanes or polysilsesquioxanes.[20−22] A very small fraction of these sorbents are being developed specifically for aldehyde capture, since amine-containing sorbents are generally suitable for this purpose because of the high reactivity of the aldehydes toward the amine group, resulting in the imine (Schiff base) linkages.[23,24] Although relatively high amine loadings can be achieved with the aminosilicas and amine-impregnated silica sorbents,[22] the increase in the amine content of the sorbents usually comes at the expense of surface area and pore volume available for sorption.

In the present work, we designed amino-containing sorbents based on MOFs that were specifically tailored for aldehyde

Received: February 6, 2013
Accepted: May 3, 2013
Published: May 14, 2013

   dx.doi.org/10.1021/am400494y | ACS Appl. Mater. Interfaces 2013, 5, 5468−5477

capture. Two MOFs of this study are frameworks based on trimeric Al^{3+} clusters and 2-aminoterephthalic acid (2-ATA) as an organic linker resulting in a robust mesoporous crystalline material. Amino moieties in the organic linker act as Brønsted bases and Al^{3+} metal centers act as Lewis acid catalytic sites.[25] Simple solvothermal routes of synthesis were employed resulting in crystal topologies designated MIL-101 and MIL-53, which have been previously resolved.[26] Because of the presence of free primary amino group in every linker molecule, the NH_2MIL101(Al) and NH_2MIL53(Al) materials possess high amino group contents. Further, they possess BET surface area in the range from 500 to 2000 m^2/g, far exceeding the surface area of most aminosilica materials.[24,25] Because the Lewis acidity of the Al^{3+} metal centers is known to be mild, we aimed at enhancing it by incorporating superacidic polyoxometalate molecules of phosphotungstic acid (PTA) into the MOF structure. We have recently reported heteropolyacid molecules to be strong catalysts of aldehyde condensation,[14] and that PTA incorporation into the amino-MOFs leads to the structures that exhibit high stability and minimal PTA leaching into a liquid environment because of the amino group-acid complexation.[27] We thus synthesized MOF/PTA composite materials that were discovered to be efficient in capturing and polymerizing aldehyde vapors as well as being heterogeneous catalysts of the aldol condensation of aldehydes in liquids.

EXPERIMENTAL SECTION

Materials. 2-Aminoterephthalic acid (99%, 2-ATA), aluminum chloride hexahydrate (99%), acetaldehyde (≥99.5%), acrolein (≥99%, anhydrous), butyl aldehyde (99%, dry), and N,N-dimethylformamide (DMF, 99.9%) were all obtained from Sigma-Aldrich Chemical Co. and used as received. All other chemicals, solvents and gases were of the higher purity available and were received from commercial sources.

MOF Synthesis. *NH_2-MIL-101(Al).* A solution of aluminum chloride hexahydrate (0.51 g, 2 mmol) and 2-ATA (0.56 g, 3 mmol) in DMF (40 mL) was kept at 130 °C for 72 h in a Teflon-lined autoclave bomb. Then the solids were separated from the solution by centrifugation (5000 *g*, 10 min) and washed with DMF under sonication for 20 min. This was followed by washing with methanol at room temperature, washing with excess hot (70 °C) methanol for 5 h, and drying under vacuum at 80 °C until constant weight was achieved. Elemental anal. Calcd (for unit cell, $Al_{816}C_{6528}H_{4896}N_{816}O_{4352}$): Al, 11.8; N, 6.13%. Found: Al, 12.1; N, 6.34%. The resulting MOF was designated NH_2MIL101(Al)$_{auto}$.

NH_2MIL53(Al). This material was synthesized by thermal treatment of the MOF components by either autoclaving or applying microwave radiation. In the autoclaving method, a solution of aluminum chloride hexahydrate (2.55 g, 10 mmol) and 2-ATA (2.8 g, 15.5 mmol) in DMF (99.9%, 40 mL) was kept at 130 °C for 72 h in a Teflon-lined autoclave bomb. The solids were separated from the solution by centrifugation (5,000 *g*, 10 min) and washed with DMF under sonication for 20 min. This was followed by washing with methanol at room temperature, washing with excess hot (70 °C) methanol for 5 h, and drying under vacuum at 80 °C until constant weight was achieved. Elemental anal. Calcd (for unit cell, $Al_4C_{32}H_{24}N_4O_{20}$): Al, 12.1; N, 6.27%. Found: Al, 12.7; N, 6.75%. The resulting MOF was designated NH_2MIL53(Al)$_{auto}$.

In a typical microwaving method, a solution of aluminum chloride hexahydrate (0.51 g, 2 mmol) and 2-ATA (0.56 g, 3 mmol) in DMF (99.9%, 40 mL) was placed in a microwave oven (Discover SP-D, CEM Corp.) and was kept at 130 °C for 1 h using microwave power of 300 mW. The solids were separated from the solution by centrifugation (5,000 *g*, 10 min) and washed with DMF under sonication for 20 min. This was followed by washing with methanol at room temperature, washing with excess hot (70 °C) methanol for 5 h, and drying under vacuum at 80 °C until constant weight was achieved. In separate series of experiments, $AlCl_3.6H_2O$ and 2-ATA concentrations were varied, while maintaining a 2:3 initial molar ratio. Elemental anal. Calcd (for unit cell, $Al_4C_{32}H_{24}N_4O_{20}$): Al, 12.1; N, 6.27%. Found: Al, 12.1; N, 6.30%. The resulting MOF was designated NH_2MIL53(Al)$_{MW}$. We were unable to obtain NH_2MIL101(Al) MOF structures utilizing the microwave oven.

Amino-Containing MOF Functionalized by Phosphotungstic Acid (PTA). Two methods of PTA incorporation into the MOF were explored: impregnation of the already prepared MOF with an aqueous solution of PTA and heating of a mixture of the MOF components and PTA (joint heating). The latter technique was explored by two methods of heat supply: conventional autoclave oven and microwave.

Impregnation. In the "impregnation" method, 0.5 g of dry NH_2MIL101(Al) synthesized in autoclave as described above was suspended in water/methanol (1:1, v/v) solution of phosphotungstic acid (0.5 g PTA in 5 mL). Aqueous/methanol PTA solutions possessed a pH of ~1, resulting in complexation between the cationic NH_2MIL101(Al) and the PTA. The suspension was sonicated and shaken at 300 rpm for 8 h. The solids were separated by centrifugation, repeatedly washed by methanol and water (pH adjusted to 4.2) and dried under vacuum. The resulting MOF was designated NH_2MIL101(Al)/PTA$_{imp}$. Elemental anal. (wt %): C, 29.1; Al, 8.20; W, 23.6. On the basis of the elemental analysis results and molecular weight of hydrated PTA ($H_3PW_{12}O_{40}\cdot 6H_2O$, W content, 73.8%; MW, 2988 Da), we estimated the PTA content of the NH_2MIL101(Al)/PTA$_{imp}$ materials to be approximately 107 μmol/g of dry powder, or 32 wt %.

An impregnation, washing and drying procedure identical to that described above was performed with MOF NH_2MIL53(Al)$_{auto}$ resulting from the autoclaving preparation method. Elemental anal. (wt %): C, 31.8; Al, 8.92; W, 21.4. On the basis of the elemental analysis results and molecular weight of hydrated PTA ($H_3PW_{12}O_{40}\cdot 6H_2O$, W content, 73.8%; MW, 2988 Da), we estimated the PTA content of the NH_2MIL53(Al)/PTA$_{imp}$ materials to be approximately 97 μmol/g of dry powder, or 29 wt %.

The content of hydrated PTA, or *P*, was calculated according to the formula, P (μmol/g) = 1×10^6(W content in the hybrid material, %)/(2988 × 73.8%).

Joint Heating. To obtain the MOF/PTA hybrid by a solvothermal method using the autoclave oven, we developed the following procedure. Aluminum chloride hexahydrate (0.51 g, 2.1 mmol), 2-amino terephthalic acid (0.56 g, 3.1 mmol), and phosphotungstic acid hydrate (250 mg, 0.086 mmol) were dissolved in DMF (30 mL) and the mixture was kept without stirring at 130 °C in a Teflon-lined autoclave bomb for 72 h. The resultant solids were separated by centrifugation, kept in methanol at 70 °C overnight, separated, washed with acetone and dried at 80 °C overnight. The resulting MOF was designated NH_2MOF(Al)/PTA$_{auto}$. It must be noted that the XRD pattern of the solid structure resulting from the autoclaving of the MOF components and PTA did not resemble that of NH_2MIL101(Al) or NH_2MIL53(Al), and hence, we used the above designation.

To obtain the MOF/PTA hybrid by a solvothermal method involving microwaving[27] of a mixture of the MOF components and PTA, we dissolved $AlCl_3\cdot 6H_2O$ (507 mg, 2.1 mmol), 2-amino-terephthalic acid (564 mg, 3.1 mmol), and PTA hydrate (985 mg, 0.34 mmol) in anhydrous N,N-dimethylformamide (DMF) and the resulting solution was brought, under constant stirring, from ambient temperature to 130 °C within 5 min followed by 1 h heating at 130 °C enabled by 300 mW power supply. The resulting solids were separated by centrifugation, kept in methanol at 70 °C overnight, separated and dried at 70 °C until constant weight. The resulting MOF was designated NH_2MIL53(Al)/PTA$_{MW}$.

METHODS

General. MOF surface area and pore parameters were measured using a Micromeritics ASAP 2020 Accelerated Surface Area and Porosimetry Analyzer (Micromeritics Corp., Norcross, GA). Thermogravimetric analysis (TGA) and simultaneous differential scanning calorimetry (DSC) were conducted using a Q600 TGA/DSC instrument (TA Instruments, Inc.). Samples were subjected to heating scans (20 °C/min) in a temperature ramp mode. TEM was performed using a JEOL-2010 Transmission Electron Microscope at an

accelerating voltage of 200 kV. Samples were prepared by placing a few drops of the MOFs dispersed in ethanol onto carbon-coated 200 mesh copper grids by Electron Microscopy Sciences. A FEI/Philips model XL30 high-brightness Field emission gun environmental scanning electron microscope was used to measure elemental composition of samples and for elemental imaging. To study distribution of PTA within the sample, a JEOL 5910 scanning electron microscope was used. Samples were magnified up to 2300 times and energy-dispersive X-ray spectroscopy (EDX) was at different positions performed on the sample. Data was collected for the large area spectra for 3 min to obtain a significant count number. The spectra were analyzed using the QUANTAX software (Bruker) with automatic region specification, and the elements analyzed were carbon, oxygen, tungsten, aluminum, phosphorus, and nitrogen.

X-ray powder diffraction (XRD) patterns were acquired for 24 h with a Panalytical X'Pert Pro multipurpose diffractometer equipped with an X'celerator high-speed detector coupled with a Ni β-filter and using the Cu Kα radiation at room temperature. Samples were packed in a ZBH placeholder. Programmable divergence slits were used to illuminate a constant length of the samples (4 mm). The published XRD pattern for MIL-101 was used as the reference pattern. Peak assignment and structure refinement were accomplished with X'Pert Highscore Plus v3 software.

Capture and Condensation of Aldehyde Vapors on MOF Materials. For aldehyde capture, borosilicate glass vials, each containing a weighed amount of dry powder of a solid sample were placed next to an open 5 mL wide mouth jar containing 2 g of liquid aldehyde, initially poured into the dish at −20 °C. Both the vials and the jar were situated in a small glass desiccator, which was sealed immediately after pouring liquid aldehyde into the jar. Aldehyde evaporated from the jar at room temperature, with the vapors contained inside of the sealed desiccator. The open vials were kept in the desiccator for 24 h to 14 days at room temperature, and the uptake of aldehyde was obtained by periodically by withdrawing the vials from the desiccator, immediately sealing them and measuring their weight. Liquid aldehyde was added to the jar within the desiccator each time the desiccator was open for the sample withdrawal, to maintain the saturated vapor atmosphere inside the desiccator. Equilibrium weight uptake was reached after 24 h, at which point no further weight increase of the vials was observed. Within 2−3 days, samples exhibited a change in color from white to yellow to brown to black in the case of acetaldehyde condensed in the vials containing NH_2MIL101(Al)/PTA_{imp} and NH_2MIL53(Al)/PTA_{imp} samples; analogous color changes were significantly slower, over 14−30 days, with other samples. The weight uptake, measured in triplicates, was calculated as WU, % = 100 × (sample weight after equilibration − initial sample weight)/initial sample weight.

Analysis of Aldehyde Vapor−MOF Reaction Products. The vapor condensed on the samples of the study was analyzed for composition by matrix -assisted laser desorption/ionization time of flight (MALDI-TOF) mass spectrometry using an Applied Biosystems Model Voyager DE-STR spectrometer, with 2,5-dihydroxybenzoic acid (DBH) as a matrix. For analysis, the acetaldehyde products adsorbed on the solid matrix were extracted by tetrahydrofuran. The sample containing 20−30 mg of solid material was suspended in 0.5 mL of THF and vortexed for 1−2 min. Then the solids were separated using a table-top centrifuge and the supernatant was diluted 50-fold by deionized water. Thus diluted extraction product (1 μL) was added to 1 uL of the matrix and spotted. The matrix consisted of 20 mg of DHB, 500 μL of acetonitrile, and 500 μL of 0.1 wt % trifluoroacetic acid. Reaction between the MOF matrix and adsorbed and condensed acetaldehyde vapor was studied as follows. After the reaction, the MOF material was rinsed with acetonitrile, separated by centrifugation, dried under vacuum, and dissolved in 20 wt % aqueous NaOH at 5 mg/mL MOF concentration. The solution was diluted 50-fold with deionized water and 1 μL of was added to 1 μL of DHB matrix; the mixture was spotted. Additionally, the aldehyde condensation products on MOF/PTA_{imp} materials were identified in acetonitrile extracts using a Bruker Daltonics Apex IV Fourier-transform ion cyclotron resonance intrument with a 7.0 T superconducting magnet. The instrument is equipped with a Bruker/Agilent Apollo off-axis electrospray (ESI) ionization source. The capillary and end plate voltages were −3760 and −3318 V, respectively. The instrument 5-point calibrations were made using an Agilent ES Tuning Mix. The samples were injected at a flow rate of 300 μL/h using a syringe pump.

Identification and Quantification of Crotonaldehyde. Samples of acetonitrile/water (100/30 v/v) media in which the acetaldehyde-particle reaction was monitored, or MOF particles with adsorbed acetaldehyde, were subjected to crotonaldehyde identification using the method described by Spaulding et al.[28] Particles or media were placed in chilled (0−4 °C) deionized water[29] and vortexed for 10 s, followed by separation of the solids by centrifugation (15 000 *g*, 30 s). The liquids were reacted with O-(2,3,4,5,6-pentafluorobenzyl)-hydroxylamine hydrochloride (PFBHA) for 24 h at room temperature.[28] The aldehyde derivatives acidified with minute amounts of sulfuric acid were then subjected to extraction into hexane.[30] Identification was performed using an Agilent 6890N gas chromatograph coupled to a 5793N quadrupole mass spectrometer. A DB-XLB capillary column was used for separating the derivatives (5% phenyl-substituted stationary phase, 30 m length, 0.25 mm I.D., 0.25 μm film thickness; J&W Scientific, Folsom, CA). The oven temperature initially was set to 50 °C and held there for 2 min, then ramped at 5 °C/min to 150 °C, 20 °C/min to 260 °C, and 30 °C/min to 325 °C, after which it was held for another 5 min.

Electron-capture negative ionization mass spectrometry (ECNI) peaks of $[C_6F_5]^-$ (*m*/*z* 167), $[C_6F_4CH_2O]^-$ (*m*/*z* 178), $[C_6F_5CH_2]^-$ (*m*/*z* 181), $[C_6F_5CHO]^-$ (*m*/*z* 196), $[C_9H_5F_4NO]^-$ (*m*/*z* = 219), $[C_9H_6F_5NO]$- (*m*/*z*=239, acetaldehyde derivative), $[C_{11}H_7F_4NO]^-$ (*m*/*z* = 246, most intense, base peak), and crotonaldehyde derivative $[C_{11}H_8F_5NO]^-$(*m*/*z* = 266) were observed. Retention times for acetaldehyde and crotonaldehyde were 11.8 and 19.4 min, respectively.

The kinetics of crotonaldehyde formation were measured spectrophotometrically in water/acetonitrile mixtures at 25 °C using a Hewlett-Packard 845× UV−visible spectrophotometer. The experiments were performed in continuously stirred glass vials shielded from light by aluminum foil. Acetaldehyde was introduced into suspensions of NH_2MIL101(Al) or NH_2MIL101(Al)/PTA material in the solvent (20 mL) by means of a syringe, and the kinetic measurements commenced. Initial acetaldehyde concentrations varied in the range 0.02−0.2 M. The kinetic analyses were based on the absorbance of reaction mixtures in the 190−1100 nm range, measured with 0.1 mL samples of the suspensions withdrawn intermittently, diluted with the acetonitrile/water solvent and placed in quartz cells (path length, 1 cm). The samples were not returned to the reaction medium after measurement, but the error introduced by the reaction volume depletion did not exceed 10% in all measurements. The dilution of the withdrawn samples was chosen such that the absorption band at 227 nm did not reach saturation for at least 24 h. The observed reaction rate constant was found from the initial slope of the conversion (*F*) vs time plot using the following expression[31]

$$\ln(1 - F) = -k_{obs}t \quad (1)$$

where $F = \Delta A_t/\Delta A_\infty$, $\Delta A_t = A_t - A_o$ is the change of electronic absorbance (*A*) at λ = 227 nm at time *t*, A_o is the absorbance at *t* = 0, and A_∞ is the absorbance at equilibrium. On the basis of k_{obs}, the half-life is found as $\tau_{1/2} = \ln(2)/k_{obs}$, and the apparent second-order rate constant is $k'' = k_{obs}/C_a$, where C_a is the initial acetaldehyde concentration.

RESULTS AND DISCUSSION

Characterization of Aluminum Aminoterephthalate MOF and Their Composites with Phosphotungstic Acid (PTA). Synthetic routes toward amino-containing NH_2MIL101(Al) and NH_2MIL53(Al) MOFs in DMF have been reported previously by Kaptein and co-workers[27,32−34] and by us.[26] The materials obtained in the present work were characterized by powder X-ray diffraction, elemental analysis, TEM, solubility studies, nitrogen adsorption isotherms at 77 K, and TGA/DSC

in a nitrogen atmosphere with temperatures up to 1200 °C. At 25 °C, aluminum aminoterephthalate MOFs were observed to be insoluble in water at pH 3−5, methanol, ethanol, hexane and benzene even after prolonged (over 2 months) exposure; no mass loss or change in the crystal structure of the MOF was observed after drying of their suspensions. The MOF dissolved, forming clear solutions, in basic aqueous media (10−20 wt % NaOH). Particle sizes of either NH_2MIL101(Al) or NH_2MIL53(Al) were in the range of 30−100 nm, and the shape was typically octahedral (S-1). Upon drying from polar solvents such as DMF, methanol or ethanol on heating, the amino-containing MOF flocculated and formed brittle sheets, which could be redispersed in organic solvents with sonication.

We have shown previously that solvothermal syntheses, with 3−5 °C/min heating rate from room temperature to 130 °C followed by maintaining the materials in a Teflon-lined autoclave for 72 h at 130 °C result in two distinctly different crystalline MOF structures, NH_2MIL101(Al) and NH_2MIL53-(Al), depending on the initial precursor ($AlCl_3.6H_2O$) concentration.[26] At initial aluminum hexahydrate concentrations in DMF below 150−200 mM, structures characteristic of MIL-101 topology were obtained, whereas higher concentrations resulted in MIL-53 crystal topology (Figure 1). Such

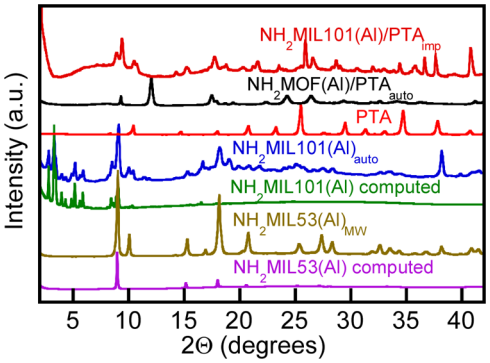

Figure 1. X-ray diffraction patterns of NH_2MIL101(Al), NH_2MIL53-(Al) MOF materials, phosphotungstic acid (PTA), and MOF/PTA hybrid materials prepared by heating MOF precursors and PTA in an autoclave (NH_2MOF(Al)/PTA_{auto}) or impregnating already prepared NH_2MIL101(Al) material with PTA solution (NH_2MIL101(Al)/PTA_{imp}). Spectra designated "computed" were computed on the basis of lattice parameters obtained from the Cambridge Structural Database (CSD) as described previously.[26]

differences are due to the kinetically controlled crystal growth,[32,35] favoring thermodynamically stable MIL-53 topology formation at higher crystal growth rates. In an effort to facilitate the MOF synthesis by microwave (MW) heating that induces rapid nucleation and crystal formation, we explored recently reported MW synthesis of the amino-functionalized MOFs,[27] while varying initial precursor concentrations and heating rates. When a suspension of 2-aminoterephthalic acid (2-ATA) and aluminum hexahydrate in DMF is MW-heated in a Teflon-lined tube from ambient temperature to 130 °C, a crystalline material is facilely obtained within the first few minutes upon reaching 100−130 °C. Powder XRD patterns indicate (Figure 1) that the materials possess the MIL-53 topology, regardless of the initial $AlCl_3{\cdot}6H_2O$ and 2-ATA concentrations, which were varied 10-fold, while maintaining a 2:3 initial molar ratio of $AlCl_3{\cdot}6H_2O$ to 2-ATA. The peak positions in the XRD spectra of $NH_2MIL53(Al)_{MW}$ were identical to those of $NH_2MIL53(Al)_{auto}$ synthesized by equilibrating the MOF/DMF suspension in an autoclave at 130 °C for 3 days and matched well the patterns of the MIL53(Al) computed using lattice parameters obtained from the Cambridge Structural Database (CSD). For computation, XRD patterns obtained from CSD for Cr-based MOF were modified by replacement of Cr with Al. Characteristic peaks belonging to $NH_2MIL53(Al)_{MW}$ were broader than in the case of $NH_2MIL53(Al)_{auto}$ because of the smaller crystallite sizes in the former. A illustrative molecular model of a NH_2MIL101-(Al)/PTA crystal unit is shown in S-2.

Functionalization of NH_2MIL101(Al) and NH_2MIL53(Al) with phosphotungstic acid (PTA) molecules was explored via multiple approaches. Heating a solution of PTA, $AlCl_3{\cdot}6H_2O$, and 2-ATA in DMF in an autoclave (130 °C, 3 days) resulted in a crystalline structure that could not be matched with either MIL-53 or MIL-101 topologies (see $NH_2MOF(Al)/PTA_{auto}$ in Figure 1). Microwaving a mixture of PTA, $AlCl_3{\cdot}6H_2O$, and 2-ATA in DMF at 130 °C for 1 h resulted in NH_2MIL53(Al) topology that contained PTA. This result is somewhat different from those published recently,[27] wherein the MIL101 topology was reported in the MOF/PTA composites obtained by microwaving at 130 °C for 1 h, but not in those kept in the autoclave for 3 days. Given these contradictory results, we focused on MOF functionalization by PTA incorporation via impregnation of already prepared MOF with PTA solutions at 25 °C (for synthesis and post-treatment detail, see the Experimental Section). It was observed that MOFs impregnated by PTA maintained their crystal topology, albeit showing increased content of the amorphous phase. Peaks belonging to the PTA crystals were also observed in NH_2MIL101(Al)/PTA_{imp} material, indicating the presence of an ordered PTA phase in the MOF/PTA composite. However, imaging of the NH_2MIL101(Al)/PTA_{imp} at magnification of 15000 x using SEM and elemental mapping did not reveal any distinct PTA phases on the surfaces of the MOF particles. Rather, relatively homogeneous distribution of PTA throughout the particles was observed (S-3).

The content of PTA in these MOF/PTA composites was high, 29−32 wt %, and PTA molecules were incorporated into the porous structure of the MOF. The relative stability of the hybrid against POM leaching out in the aqueous/organic solvent solutions (see below) can be explained by electrostatic interactions between the $[PW_{12}O_{40}]^{3-}$ Keggin ions and $-NH_3^+$ groups of the MOF. The amino groups of 2-ATA possess pK_a below 10 and are available for complexation when 2-ATA is incorporated into the Al^{3+}-based MOF structures.[26] Formation of complexes such as $-NH_3^+[H_2PW_{12}O_{40}]^-$ between primary amines, ammonia or pyridine and PTA is well-documented.[36−38] Analogously, stable electrostatic complexation between cationic silica nanoparticles and negatively charged polyoxometalates has been reported.[39−41]

TGA and DSC thermograms of the NH_2MIL101(Al) MOF samples released up to 8 wt % of solvent at temperatures ≤100 °C and decomposed only at temperatures above 450 °C, following endothermic melting of the 2-aminoterephthalic acid-Al^{3+} complexes (S-4). The thermograms of NH_2MIL101(Al)/PTA_{imp} and NH_2MIL53(Al)/PTA_{imp} were similar to those of their parent MOFs, but exhibited additional sharp, 20−23 wt % weight loss at T > 800 °C, in agreement with the reported Keggin structure decomposition at these temperatures.[42]

The specific BET surface areas of the MOFs NH_2MIL101-(Al) and NH_2MIL53(Al) of 1920 and 780 m^2/g, respectively,

dx.doi.org/10.1021/am400494y | ACS Appl. Mater. Interfaces 2013, 5, 5468−5477

were lowered 4−8-fold by incorporation of PTA molecules into the MOF pores. We will discuss the surface areas of various MOF species in more detail in what follows.

Capture and Chemical Conversion of Aldehyde Vapors by MOF and MOF/PTA Materials. Figure.2 shows BET area of the dry MOF samples and acetaldehyde vapor uptake after 48 h equilibration at 25 °C.

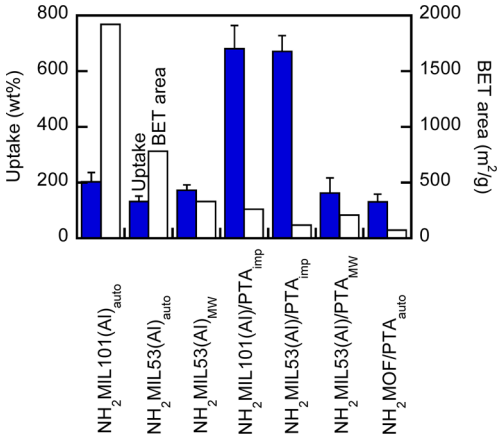

Figure 2. Acetaldehyde vapor uptake (filled columns) and BET area (open columns) of the MOF species under study. Designations "auto" and "MW" stand for the solvothermic syntheses in the autoclave and microwave oven, respectively. Designation "imp" stands for impregnation of the respective MOF material with PTA solution as described in the Experimental Section.

All samples exhibited a significant uptake of acetaldehyde from its vapor phase, exceeding 50 wt % in all cases. For comparison, the acetaldehyde uptake values calculated based on the measured BET surface area, assumption of the monomolecular adsorption, and the cross-sectional area of the acetaldehyde molecule (22.2 Å^2)[43] yielded 3- to 5-fold lower values than the experimentally measured ones in the case of unmodified MOFs. The uptake values were dramatically, up to 80- to 160-fold lower values in the case of the MOFs modified by impregnation with PTA. This clearly shows that the acetaldehyde vapor uptake occurs through the vapor condensation mechanism, which depends on the chemical nature of the materials. Using Crystal Maker software and unit cell models,[26] we computed the void volume and density of NH_2MIL101(Al) to be 95.1% and 450.6 kg/m^3, respectively, while for the NH_2MIL53(Al) MOF we obtained 88.9% and 982.1 kg/m^3, respectively. Given the density of liquid acetaldehyde of 788 kg/m^3 at standard temperature and pressure, the calculated weight uptake by the pore-filling model is 166 and 71 wt % for NH_2MIL101(Al) and NH_2MIL53(Al) MOF, respectively. These values are 1.2 to 1.8-fold higher than experimentally observed ones, indicating that acetaldehyde formed a liquid phase on the MOFs particle surfaces.

The liquid acetaldehyde phase, initially yellowish, became brown and viscous (caramelized) over time. The uptake of aldehyde vapors by the MOFs, even without PTA, was at least 5-fold higher than physisorption on wood origin-carbon with a BET surface area of 2266 m^2/g, chemically activated with phosphoric acid, under saturated vapor conditions.[44] Generally, acetaldehyde adsorption on activated carbons is poor, but can be enhanced by carbon oxidation followed by the appearance of the carbonyl and carboxyl groups on the surface, capable of hydrogen bonding and attractive dipole−dipole interactions with the aldehyde vapor molecules.[45,46] From a practical standpoint, amino-modified mesoporous silica materials could be higher-capacity sorbents for aldehydes than activated carbons, where the uptake, directly proportional to the content of the accessible amino groups, occurs primarily via the formation of imines through the aldehyde-amine reaction.[23,24] The superiority of the amino-containing MOFs versus the aminosilica materials in aldehyde uptake stems from the differences in uptake mechanisms. The adsorption performance of the aminosilicas depends on their primary amino group content; the sorption capacity does not reach equimolar aldehyde-to-amine group due to the $-NH_2$ group accessibility limitations.[24] On the other hand, the uptake of acetaldehyde was measured to be 30 and 45 mequiv/g for NH_2MIL101(Al) and NH_2MIL53(Al) MOFs, respectively, which was 5- to 10-fold higher than the content of the amino groups in aminosilicas (4.5−5.2 mequiv/g). We were able to detect the imine products of the reaction between sorbed acetaldehyde and $-NH_2$ groups of the MOF (S-5), in a reaction analogous to that in formaldehyde sorption on alumosilicas.[24]

The aldehyde uptake by the MOFs exceeding the amino group content can be potentially explained by the Brønsted and Lewis acidity of the aluminum carboxylate clusters,[47,48] which cause aldolization of the sorbed acetaldehyde to crotonaldehyde, followed by aldolization of the latter with acetaldehyde, etc.[49] The effects of the acid presence on the conversion of the sorbed aldehyde are discussed in greater detail in what follows.

It is interesting to note that the NH_2MIL101(Al)/PTA$_{imp}$ and NH_2MIL53(Al)/PTA$_{imp}$ MOFs modified by PTA using impregnation in the presence of water demonstrated a 5−10-fold higher acetaldehyde uptake compared with the rest of the materials of this study (Figure.2). These composite materials possess identifiable crystalline phases of PTA, at variance with the NH_2MIL53(Al)/PTA$_{MW}$ and NH_2MOF/PTA$_{auto}$ where PTA is molecularly dispersed. It appears that the impregnated species with PTA crystals were far stronger Lewis acids than the other MOF/PTA materials due to the presence of superacidic PTA molecules. These results are analogous to the ones in our previous work with MIL101(Cr)/PTA composite materials, where PTA molecules (themselves superior catalysts of the aldol condensation of acetaldehyde) were incorporated into the chromium(III) terephthalate MOF without changes in the PTA acidity or structure.[49,50]

Using mass spectroscopy, we identified the main products of the acetaldehyde vapor condensation catalyzed by the MOF/PTA$_{imp}$ composite materials. The identified compounds are presented in Table 1. A representative MALDI-TOF spectrum of the extract of the acetaldehyde vapor-NH_2MIL101(Al)/PTA$_{imp}$ reaction products is shown in Figure 3.

Analogously, electrospray ionization spectroscopy (S-6,S-7) allowed for positive identification of the acetaldehyde condensation products [M-H$^+$] listed in Table 1. These results unequivocally point out to the repeated aldol condensation, eventually producing polymeric species (Figure.4).[14,49,50]

The uptake of saturated vapors of acrolein and butyraldehyde by the MOF and MOF/PTA$_{imp}$ materials shown in Figure 5 was much less pronounced than that of acetaldehyde, in sequence acetaldehyde ≫ acrolein > butyraldehyde. The uptake of acrolein by MOF or MOF/PTA exceeded several-fold saturation adsorption capacity of heat-activated 3A molecular sieves (synthetic zeolite), measured to be ∼25% under saturated vapor conditions.[51]

Table 1. Acetaldehyde Condensation Products Identified in MALDI-TOF Spectra of THF Extracts from NH_2MIL101(Al)/PTA_{imp} Sample Equilibrated with Acetaldehyde Vapor at 25 °C for 48 h

Number	Chemical name	Structure	Observed m/z
1	2,4-dimethyl crotonaldehyde		97.4
2	3-hydroxy-2-methylpentanal	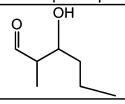	115.4
3	(*E*)-2,5-dimethylhexa-2,4-dienal	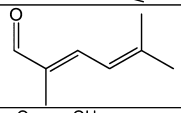	123.4
4	3-hydroxy-2,5-dimethylhex-4-enal	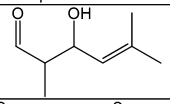	141.5
5	(E)-2,3-dimethyl-5-oxooct-6-enal	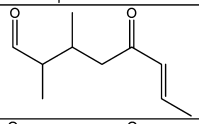	167.4
6	7-hydroxy-2,3-dimethyl-5-oxooctanal	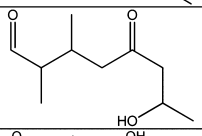	185.4
7	(3E,5E)-5-hydroxy-2,3-dimethyl-7-oxonona-3,5,8-trienal	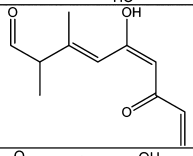	193.5
8	(E)-6-hydroxy-3,4,5-trimethylnon-3-ene-2,8-dione	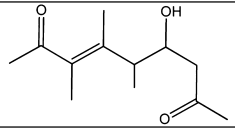	211.6

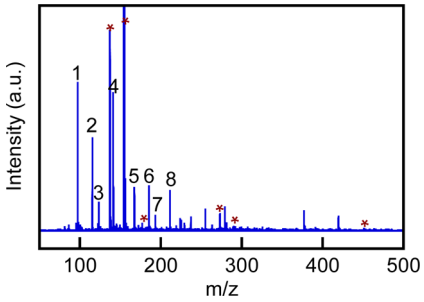

Figure 3. MALDI-TOF spectrum of the reaction product extract from NH_2MIL101(Al)/PTA_{imp} sample equilibrated with acetaldehyde vapor at 25 °C for 48 h. Asterisk shows peaks belonging to the DHB matrix, whereas numbers designate identified compounds of acetaldehyde conversion (see Table 1).

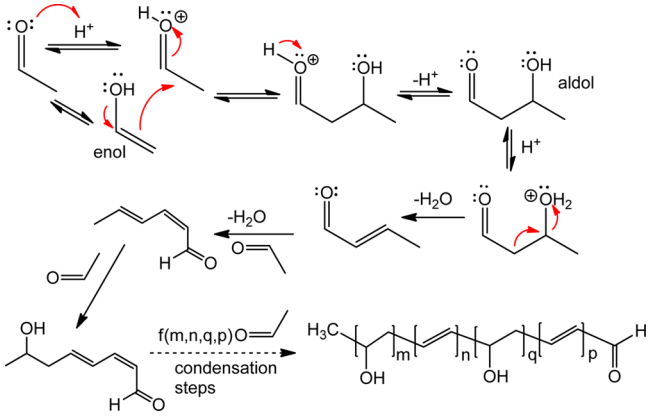

Figure 4. Mechanism of repeated, acid-catalyzed aldol condensation of acetaldehyde.

It is interesting to observe that while the overall uptake of butyraldehyde was enhanced by the presence of PTA in the MOF materials, the uptake of acrolein by the MOF/PTA composites was smaller than that by the parent MOFs. These differences in the effect of PTA presence on the vapor uptake can be explained as follows. The sorbed vapor of butyraldehyde undergoes repeated acid-catalyzed aldol condensation and dehydration, as supported by the identification of its condensation products extracted from the MOF/PTA (S-8,S-9). Products such as (Z)-oct-4-enal (m/z = 126.1), 5-hydroxyoctanal (m/z = 144.1), dihydroxydodecanal (m/z = 216.2), dodecanal (m/z=184.2), dehydrogenated palmitaldehyde (m/z = 238−240), etc. were found. Similarly to the case of acetaldehyde, the mixture of condensation products of butyraledhyde is a liquid, the formation of which is enhanced by the superacidic PTA molecules.

On the other hand, acrolein visibly polymerized on the MOF/PTA over the course of our experiments, forming higher molecular weight and eventually, solid products. Such products evidently blocked access of the incoming acrolein vapor molecules, thereby limiting further uptake. Formation of a

dx.doi.org/10.1021/am400494y | ACS Appl. Mater. Interfaces 2013, 5, 5468−5477

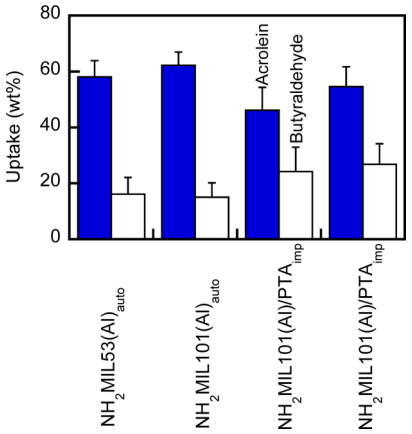

Figure 5. Equilibrium acrolein (filled columns) and butyraldehyde (open columns) vapor uptake by MOF species. Designations "auto" and "imp" stand for the solvothermic syntheses in autoclave impregnation of the MOF material with PTA solution as described in Experimental Section.

solid brownish mass was observed wherein the discrete MOF particles were hardly distinguishable. Despite the polymerization and formation of solid cross-linked structures, we were able to extract some of the products from the MOF/PTA material and identify them in the ESI mass spectra (S-10, S-11). Polymerization products such as 2-ethyl-5-methylhexanedial (m/z = 156.1), 3-methyldecane-2,5,8-tricarbaldehyde (m/z = 240.2), 3-ethyl-6-methyloctahydropyrano[2,3-b]pyran-2,7-diol (m/z = 216) were identified, which confirmed the mechanism of polymerization (Figure 6), wherein the acid-catalyzed

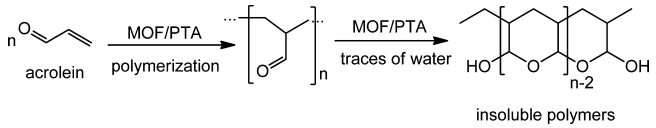

Figure 6. Polymerization of acrolein sorbed on MOF/PTA composite materials.

dehydration was a possible source of water traces. The as-obtained polyacrolein is highly cross-linked through intermolecular acetal linkages.[52−54] The phenomenon of acrolein polymerization (Figure 6) through 1,2- or 1,4-additions is well-known and can be spontaneous or initiated by oxidation catalysts such as polyoxometalates or by organic bases,[54−57] although the mechanism of such reactions has not been elucidated in detail and is very difficult to ascertain.

It is interesting to note that a gas-phase production of acrolein by dehydration of glycerol catalyzed by strong acids, including PTA and other heteropolyacids supported on silica, titania, alumina or zirconia is well-developed due to its potential for sustainable production of chemicals from renewable biomass.[58−62] However, at high temperatures typically employed in such processes to gasify glycerin (>250−300 °C), the produced acrolein does not polymerize.

To summarize, we determined the high sorption capacity of the amino-containing MOF and their composites with PTA for aldehydes and suggested reactivity mechanisms, in the reactive depletion of the aldehydes by aldol condensation and polymerization at ambient temperature.

Kinetics and Mechanism of Aldol Condensation of Acetaldehyde Catalyzed by MOF and MOF/PTA Composites Dispersed in Liquid Milieu. As we have shown above, aldehydes sorbed on aluminum aminoterephthalate MOFs and their composites with PTA from the aldehyde-saturated vapor phase underwent aldol condensation followed by the formation of higher molecular weight products. Using the mass spectroscopy method described in the Experimental Section, we detected the presence of crotonaldehyde in the acetaldehyde vapors adsorbed onto NH_2MIL101(Al) and NH_2MIL101(Al)/PTA_{imp} materials approximately 0.5 h after the start of exposure of these materials to the vapors. However, because of the uncertainty in the crotonaldehyde quantification and because of the complex nature of the adsorption from the vapor phase that is followed by the (transport-limited) sorbent−sorbate reactions, we were unable to quantify the kinetics of acetaldehyde condensation upon adsorption from the vapor phase. The acetaldehyde reaction kinetics can be readily followed in agitated liquid media when liquid acetaldehyde is injected instantly into the medium. It has been shown that oligomerization of acetaldehyde in aqueous solutions and organic solvents catalyzed by amino acids is illustrative of the processes occurring in atmospheric aerosols.[63] In the present work, we studied the kinetics of the MOF-catalyzed aldol condensation in water-acetonitrile mixtures, as they appeared to be most appropriate for the electronic absorption assays because of their optical transparency, full miscibility with acetaldehyde, and nondissolving nature toward NH_2MIL101(Al) and NH_2MIL101(Al)/PTA materials, which showed no leaching of any optically detectable components even after prolonged (several weeks) exposure. Representative electronic absorption spectra are shown in S-12. The absorption maximum at 227 nm corresponds to crotonaldehyde,[63] the presence of which was confirmed independently by mass spectrometry (see Experimental Section). Broader maxima at 260 and 280 nm due to the carbonyl absorption are attributable to both acetaldehyde and *trans*- and *cis*-crotonaldehyde, as well as to the presence of other carbonyl-containing compounds,[63,64] and therefore cannot be utilized for the monitoring aldol condensation kinetics. With no catalyst, the solution of acetaldehyde in the same water/acetonitrile medium was stable for at least 24 h, with the absorption maximum at 280 nm (S-12).

The aldol condensation rates in MOF suspensions were relatively rapid and followed pseudofirst order reaction kinetics (linear fits to eq 1; Figure 7). Without the catalysts, no formation of crotonaldehyde was observed under identical conditions.

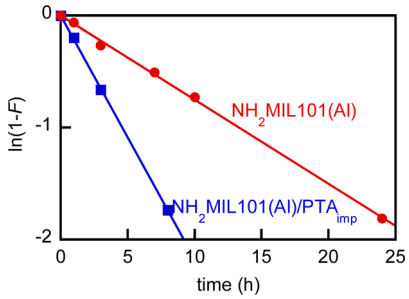

Figure 7. Kinetics of crotonaldehyde evolution in 10 mg/mL suspensions of NH_2MIL101(Al)/PTA_{imp} and NH_2MIL101(Al) in water/acetonitrile (30:70 v/v) media at 25 °C. Initial acetaldehyde and MOF concentrations are 0.18 M and 10 mg/mL, respectively. F is the conversion.

Interestingly, both the MOF/PTA composite and MOF itself catalyzed formation of crotonaldehyde, with the observed rate constants (k_{obs}) estimated to be 6.0×10^{-5} and 2.1×10^{-5} s^{-1}, respectively. Both the proton-donating PTA and the primary amino groups of NH_2MIL101(Al) can accelerate the aldol condensation of acetaldehyde in the presence of water, analogously to the previously reported catalysis of aldol condensation of acetaldehyde by amino acids.[63] An approximately 3-fold slower kinetics with NH_2MIL101(Al) material could be related to the rate-limiting step of enamine or iminium formation via Mannich condensation mechanism (Figure 8), which may not be prominent with NH_2MIL101(Al)/PTA_{imp}, where the acid-catalyzed reaction (Figure 4) dominates.

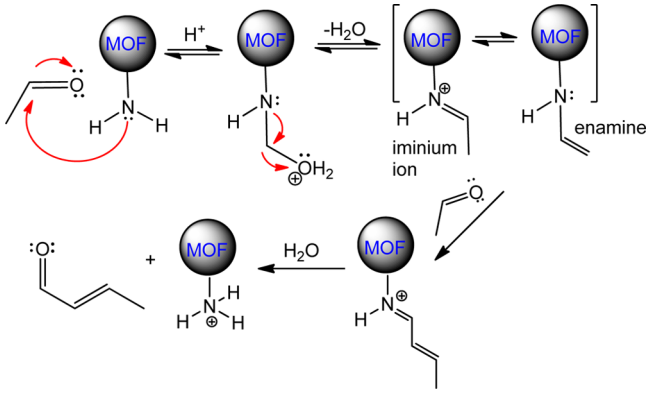

Figure 8. Mannich pathway of acetaldehyde condensation catalyzed by the amino groups of the MOF belonging to 2-aminoterephthalic acid linker.

The half-life ($\tau_{1/2}$) values estimated herein to be 3.2 and 9.4 h in the case of NH_2MIL101(Al)/PTA_{imp} and NH_2MIL101-(Al), respectively, were approximately 5−10-fold shorter than those for acetaldehyde condensation in water catalyzed by amino acids, as well as those in 75−80 wt % sulfuric acid.[31,6566] By varying initial acetaldehyde concentrations in the 0.02−0.2 M range, linear dependencies of the k_{obs} on the initial acetaldehyde concentration (C_a) were found (Figure 9), in agreement with the previous reports on homogeneous catalysis by amino acids.[63]

The apparent second-order rate constants (k'') found from the slopes of the linear k_{obs} *vs* C_a fits in Figure.9 were 1.5×10^{-3} and 5×10^{-4} M^{-1} s^{-1} for NH_2MIL101(Al)/PTA_{imp} and NH_2MIL101(Al) materials, respectively. These constants were approximately 10-fold higher than those reported in the case of homogeneous catalysis by amino acids.[63] To address the question regarding the potential recovery of our catalytic materials and their reuse, which might be affected by the poisoning of the catalytic amine groups of the MOF through their Mannich reaction with acetaldehyde (Figure 8), we tested catalytic performance of NH_2MIL101(Al)/PTA_{imp} and NH_2MIL101(Al) materials in three consecutive cycles, under conditions identical to those reported above (see Figure 9). After 24 h kinetics, the solids were recovered from the suspensions by centrifugation (10 000 rpm, 3 min), washed by excess water/acetonitrile (30:70 v/v) medium and dried under vacuum. Thus recovered solids were utilized in the next cycle. Within the experimental error (15%), no loss of catalytic activity in three consecutive cycles was observed in either case. The observed formation of the imine products of the acetaldehyde vapor reaction with the amino groups belonging to 2-aminoterephthalic acid of the MOF (S-5) did not impede the MOF reuse in the liquid medium. In order to dissolve the MOF in water for the MALDI-TOF analysis, we employed a strongly basic (20 wt % NaOH) aqueous solution. Addition of the base in these experiments can stabilize the iminium ions, which prevented the hydrolysis of the ethylideneamino terephthalic acid and other imine products of the acetaldehyde reaction with amine groups, identified by MALDI. On the other hand, the water/acetonitrile mixture employed in the catalytic turnover enabled enamine hydrolysis (Figure.8), thus "liberating" the catalytic amino groups of the MOF and permitting the catalyst reuse. Further, we conducted a control series of experiments wherein the NH_2MIL101(Al)/PTA_{imp} or NH_2MIL53(Al)/PTA_{imp} materials were suspended at 10 mg/mL concentration in the water/acetonitrile (30:70 v/v) solvent, briefly sonicated and shaken at 200 rpm at 25 °C for 8 h. The resulting suspensions were cleared of solids by filtration as described previously[50] and the supernatants were mixed with acetaldehyde and subjected to the kinetic study as described above (Figure 7). The observed rate constants (k_{obs}) were below 1×10^{-7} s^{-1}, as in the control water/acetonitrile (30:70 v/v) solvent that had not been in contact with the MOF/PTA materials. These experiments demonstrated that the MOF/PTA materials themselves, and not the PTA that could potentially leach out, catalyzed the aldehyde conversion. That is, we discovered MOF and MOF/PTA nanoparticles are efficient heterogeneous catalysts for the aldehyde self-condensation in the aqueous−organic media.

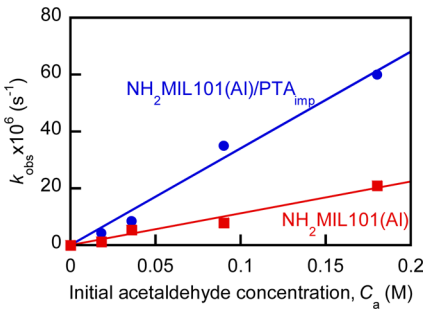

Figure 9. Observed initial rate constants of crotonaldehyde evolution as a function of initial acetaldehyde concentrations (C_a). Conditions: 10 mg/mL suspensions of NH_2MIL101(Al)/PTA_{imp} and NH_2MIL101(Al) in water/acetonitrile (30:70 v/v) media at 25 °C.

CONCLUDING REMARKS

Thus far, reactive sorbents for removal of aldehyde vapors from air and liquid media have been based primarily on amino-containing materials such as mesoporous aminosilica, where aldehyde sorption occurs via irreversible aldehyde-amine reaction. In the present work, we introduced a concept of the amino-containing MOF with surface areas and functional group contents exceeding those of the typical mesoporous aminosilica. The aminoterephthalate-based MOFs and their composites with heteropolyacid simply impregnated into and electrostatically complexed with the MOF surface appeared to be extremely efficient sorbents of volatile aldehydes. Addition of PTA imparts acidic functionality to the MOF and enhances acetaldehyde and butyraldehyde vapor uptake due to the enhancement of the aldol condensation of the sorbed aldehyde molecules. Repeated aldol condensation leads to the appearance of oligomeric and polymeric products, which are by far

less volatile than the parent acetaldehyde. Acrolein vapors are eliminated from air because of their vinyl polymerization with products that eventually solidify the sorbent/sorbate mixture. In liquid medium, the amino groups belonging to both the MOF and PTA catalyze the acetaldehyde conversion to crotonaldehyde, either through the Mannich pathway or via aldol condensation. The kinetics of such conversion with the MOF/PTA composite appear to be very fast, with half-lives of approximately 3.2 h, which are 5−10-fold shorter than those for acetaldehyde condensation in water catalyzed by 80 wt % sulfuric acid. However, unlike the liquid acid, MOF/PTA is shown to be a recyclable catalyst for the acetaldehyde conversion. An additional advantage of the amino-containing MOFs is that they can be engineered into various designs of reactive filters because of the presence of the amino groups allowing for covalent attachment of the MOF particles to solid surfaces.

■ ASSOCIATED CONTENT

Ⓢ Supporting Information

TEM and SEM images of MOF, TGA, and DSC thermograms; MALDI-TOF and electrospray ionization mass spectra and structures of identified products; physical properties and structure of studied aldehydes; electronic absorption spectra illustrating kinetics of aldol condensation. This material is available free of charge via the Internet at http://pubs.acs.org.

■ AUTHOR INFORMATION

Corresponding Author

*E-mail: tahatton@mit.edu.

Notes

The authors declare no competing financial interest.

■ ACKNOWLEDGMENTS

The authors are grateful to Dr. Scott A. Speakman (Department of Materials Science and Engineering, MIT) for help with XRD experiments and interpretation, Ms. Li Li (Department of Chemistry, MIT) for help with mass spectrometry, and Mr. Patrick Boisvert (Center for Materials Science and Engineering, MIT) for help with electron microscopy. This research was funded, in part, by Philip Morris International; however, the opinions and conclusions do not necessarily reflect the position of Philip Morris International.

■ REFERENCES

(1) Tanabe, K. K.; Cohen, S. M. *Inorg. Chem.* **2010**, *49*, 6766−6774.
(2) Schröder, F.; Fischer, R. A. *Top. Curr. Chem.* **2010**, *293*, 77−113.
(3) Ranocchiari, M.; van Bokhoven, J. A. *Phys. Chem. Chem. Phys.* **2011**, *13*, 6388−6396.
(4) Bradshaw, D.; Garai, A.; Huo, J. *Chem Soc Rev.* **2012**, *41*, 2344−2381.
(5) Gu, Z. Y.; Wang, G.; Yan, X. P. *Anal. Chem.* **2010**, *82*, 1365−1370.
(6) Zhang, W.; Huang, H.; Zhong, C.; Liu, D. *Phys. Chem. Chem. Phys.* **2012**, *14*, 2317−2325.
(7) Stock, N.; Biswas, S. *Chem. Rev.* **2012**, *112*, 933−969.
(8) Li, J.-R.; Sculley, J.; Zhou, H.-C. *Chem. Rev.* **2012**, *112*, 869−932.
(9) Sumida, K.; Rogow, D. L.; Mason, J. A.; McDonald, T. M.; Bloch, E. D.; Herm, Z. R.; Bae, T.-H.; Long, J. R. *Chem. Rev.* **2012**, *112*, 724−781.
(10) Lee, J.-Y.; Farha, O. M.; Roberts, J.; Scheidt, K.; Nguyen, S. T.; Hupp, J. T. *Chem. Soc. Rev.* **2009**, *38*, 1450−1459.
(11) Ma, L.; Abney, C.; Lin, W. *Chem. Soc. Rev.* **2009**, *38*, 1248−1256.
(12) Corma, A.; Garcia, H.; Llabres, F. X.; Xamena, I. *Chem. Rev.* **2010**, *110*, 4606−4655.
(13) Yoon, M.; Srirambalaji, R.; Kim, K. *Chem. Rev.* **2012**, *112*, 1196−1231.
(14) Bromberg, L.; Hatton, T. A. *ACS Appl. Mater. Interfaces* **2011**, *3*, 4756−4764.
(15) Wu, P.; Cheng, He, C.; Wang, J.; Peng, X.; Li, X.; An, Y.; Duan, C. *J. Am. Chem. Soc.* **2012**, *134*, 14991−14999.
(16) *Agency for Toxic Substances and Disease Registry (ATSDR)*; U.S. Public Health Service: Atlanta, GA, 1990.
(17) Ghilarducci, D. P.; Tjeerdema, R. S. *Rev. Environ. Contam. Toxicol.* **1995**, *144*, 95−146.
(18) Seaman, V. Y.; Charles, M. J.; Cahill, T. M. *Anal. Chem.* **2006**, *78*, 2405−2412.
(19) Feng, Y.; Mu, C.; Zhai, J.; Li, J.; Zou, T. J. *Hazard. Mater.* **2010**, *183*, 574−582.
(20) Hicks, J. C.; Drese, J. H.; Fauth, D. J.; Gray, M. L.; Qi, G.; Jones, C. W. *J. Am. Chem. Soc.* **2008**, *130*, 2902−2903.
(21) Samanta, A.; Zhao, A.; Shimizu, G. K.H.; Sarkar, P.; Gupta, R. *Ind. Eng. Chem. Res.* **2012**, *51*, 1438−1463.
(22) Choi, S.; Drese, J. H.; Eisenberger, P. M.; Jones, C. W. *Environ. Sci. Technol.* **2011**, *45*, 2420−2427.
(23) Sae-ung, S.; Boonamnuayvitaya, V. *Environ. Eng. Sci.* **2008**, *25*, 1477−1485.
(24) Drese, J. H.; Talley, A. D.; Jones, C. W. *ChemSusChem* **2011**, *4*, 379−385.
(25) Srirambalaji, R.; Hong, S.; Natarajan, R.; Yoon, M.; Hota, R.; Kim, Y.; Ko, Y. H.; Kim, K. *Chem. Commun.* **2012**, *48*, 11650−11652.
(26) Bromberg, L.; Klichko, Y.; Chang, E. P.; Speakman, S.; Straut, C. M.; Wilusz, E.; Hatton, T. A. *ACS Appl. Mater. Interfaces* **2012**, *4*, 4595−4602.
(27) Ramos-Fernandez, E. V.; Pieters, C.; van der Linden, B.; Juan-Alcañiz, J.; Serra-Crespo, P.; Verhoeven, M. W. G. M.; Niemantsverdriet, H.; Gascon, J.; Kapteijn, F. *J. Catal.* **2012**, *289*, 42−52.
(28) Spaulding, R. S.; Frazey, P.; Xin Rao, X.; Charles, M. J. *Anal. Chem.* **1999**, *71*, 3420−3427.
(29) Cancho, B.; Ventura, F. *Global NEST J.* **2005**, *7*, 72−94.
(30) Cahill, T. M.; Charles, M. J.; Seaman, V. Y. *Development and Application of a Sensitive Method to Determine Concentrations of Acrolein and Other Carbonyls in Ambient Air*; Health Effects Institute Report No. 149 ; Health Effects Institute: Boston, MA, 2010.
(31) Casale, M. T.; Richman, A. R.; Elrod, M. J.; Garland, R. M.; Beaver, M. R.; Tolbert, M. A. *Atmos. Environ.* **2007**, *41*, 6212−6224.
(32) Gascon, J.; Aktay, U.; Hernandez-Alonso, M. D.; van Klink, G. P. M.; Kapteijn, F. *J. Catal.* 2009, *261*, 75− 87.
(33) Serra-Crespo, P.; Ramos-Fernandez, E. V.; Gascon, J.; F., Kapteijn, F. *Chem. Mater.* **2011**, *23*, 2565−2572.
(34) Juan-Alcañiz, J.; Gascon, J.; Kapteijn, F. *J. Mater. Chem.* **2012**, *22*, 10102−10118.
(35) Juan-Alcañiz, J.; Goesten, M.; Martinez-Joaristi, A.; Stavitski, E.; Petukhov, A. V.; Gascon, J.; Kapteijn, F. *Chem. Commun.* **2011**, *47*, 8578−8580.
(36) Hodnett, B. K.; Moffat, J. B. *J. Catal.* **1984**, *88*, 253−263.
(37) Shiju, N. R.; Alberts, A. H.; Khalid, S.; Brown, D. R.; Rothenberg, G. *Angew. Chem., Int. Ed.* **2011**, *50*, 9615−9619.
(38) Souza, A. L.; Marques, L. A.; Eberlin, M. N.; Nascente, P. A. P.; Herrmann Junior, P. S. P.; Leite, F. L.; Rodrigues-Filho, U. P. *Thin Solid Films* **2012**, *520*, 3574−3580.
(39) Okun, N. M.; Anderson, T. M.; Hill, C. L. *J. Am. Chem. Soc.* **2003**, *125*, 3194−3195.
(40) Okun, N. M.; Ritorto, M. D.; Anderson, T. M.; Apkarian, R. P.; Hill, C. L. *Chem. Mater.* **2004**, *16*, 2551−2558.
(41) Uma, T.; Nogami, M. *Chem. Mater.* **2007**, *19*, 3604−3610.
(42) Tanada, S.; Boki, K. *Bull. Environm. Contam. Toxicol.* **1979**, *23*, 524−530.
(43) El-Sayed, Y.; Bandosz, T. J. *J. Colloid Interface Sci.* **2001**, *242*, 44−51.
(44) Belfort, G. *Environ. Sci. Technol.* **1979**, *13*, 939−946.

(45) El-Sayed, Y.; Bandosz, T. J. *Fuel Chem. Div. Prepr.* **2002**, *47*, 465.
(46) Ravon, U.; Chaplais, G.; Chizallet, C.; Seyyedi, B.; Bonino, F.; Bordiga, S.; Bats, N.; Farrusseng, D. *ChemCatChem* **2010**, *2*, 1235−1238.
(47) Dhakshinamoorthy, A.; Alvaro, A.; Garcia, H. *Adv. Synth. Catal.* **2010**, *352*, 711−717.
(48) Luo, S.; Falconer, J. L. *Catal. Lett.* **1999**, *57*, 89−93.
(49) Bromberg, L.; Hatton, T. A. *ACS Appl. Mater. Interfaces* **2011**, *3*, 4756−4764.
(50) Bromberg, L.; Diao, Y.; Wu, H.; Speakman, S. A.; Hatton, T. A. *Chem. Mater.* **2012**, *24*, 1664−1675.
(51) Gold, A.; Dubé, C. E.; Perni, I. B. *Anal. Chem.* **1978**, *50*, 1839−1841.
(52) Imoto, T.; Matsubara, T. *J. Polym. Sci., A* **1964**, *2*, 4573−4581.
(53) Ryder, E. E.; Pezzaglia, P. *J. Polym. Sci. A* **1965**, *3*, 3459−3469.
(54) Yamashita, M.; Morita, S.; Maeshima, T. *J. Macromol. Sci., Part A* **1978**, *12*, 1261−1274.
(55) Maksimchuk, N. V.; Kholdeeva, O. A.; Kovalenko, K. A.; Fedin, V. P. *Isr. J. Chem.* **2011**, *51*, 281−289.
(56) Nuyken, O. In *Handbook of Polymer Synthesis*, 2nd ed.; Kricheldorf, H. R., Nuyken, O., Swift. G., Eds.; CRC Press: Boca Raton, FL, 2004; Chapter 10.
(57) Atia, H.; Armbruster, U.; Martin, A. *J. Catal.* **2008**, *258*, 71−82.
(58) Chai, S.-H.; Wang, H.-P.; Liang, Y.; Xu, B.-Q. *Appl. Catal., A* **2009**, *353*, 213−222.
(59) Chai, S.-H.; Wang, H.-P.; Liang, Y.; Xu, B.-Q. *Green Chem.* **2007**, *9*, 1130−1136.
(60) Chai, S.-H.; Wang, H.-P.; Liang, Y.; Xu, B.-Q. *Green Chem.* **2008**, *10*, 1087−1093.
(61) Zsigmond, Á.; Bata, P.; Fekete, M.; Notheisz, F. *J. Environ. Protect.* **2010**, *1*, 201−205.
(62) Katryniok, B.; Paul, S.; Belliere-Baca, V.; Reye, P.; Dumeignil, F. *Green Chem.* **2010**, *12*, 2079−2098.
(63) Noziére, B.; Córdova, A. *J. Phys. Chem. A* **2008**, *112*, 2827−2837.
(64) Magneron, I.; Thévenet, R.; Mellouki, A.; Le Bras, G.; Moortgat, G. K.; Wirtz, K. *J. Phys. Chem. A* **2002**, *106*, 2526−2537.
(65) Baigrie, L. M.; Cox, R. A.; Slebocka-Tilk, H.; Tencer, M.; Tidwell, T. T. *J. Am. Chem. Soc.* **1985**, *107*, 3640−3645.
(66) Esteve, W.; Noziére, B. *J. Phys. Chem. A* **2005**, *109*, 10920−10928.